JACS
JOURNAL OF THE AMERICAN CHEMICAL SOCIETY

ARTICLE

pubs.acs.org/JACS

Deciphering the DNAzyme Activity of Multimeric Quadruplexes: Insights into Their Actual Role in the Telomerase Activity Evaluation Assay

Loic Stefan, Franck Denat, and David Monchaud*

Institut de Chimie Moléculaire, Université de Bourgogne (ICMUB), CNRS UMR5260, 9, avenue Alain Savary, 21000 Dijon, France

Supporting Information

ABSTRACT: The end of human telomeres is comprised of a long G-rich single-stranded DNA (known as 3′-overhang) able to adopt an unusual three-dimensional "beads-on-the-string" organization made of consecutively stacked G-quadruplex units (so-called quadruplex multimers). It has been widely demonstrated that, upon interaction with hemin, discrete quadruplexes acquire peroxidase-mimicking properties, oxidizing several organic probes in H_2O_2-rich conditions; this property, known as DNAzyme, has found tens of applications in the last two decades. However, little is known about the DNAzyme activity of multimeric quadruplexes; this is an important question to address, especially in light of recent reports that exploit the DNAzyme process to optically assess the activity of an enzyme that elongates the telomeric overhang, the telomerase. Herein, we thoroughly investigate the DNAzyme activity of long telomeric fragments, with a particular focus on both the nature of the hemin/multimeric quadruplex interactions and the putative higher-order fold of the studied fragments; in light of our results, we also propose possible ways that may be followed to improve the use of DNAzyme to evaluate the telomerase activity.

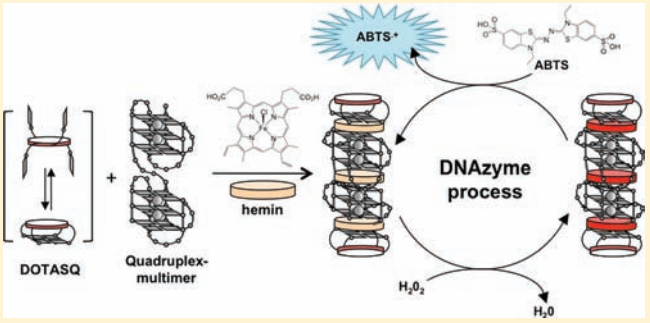

INTRODUCTION

The repetitive $(TTAGGG)_n$ nature of the DNA component of the human telomeres, the nucleoproteic assembly that molds and protects the end of the chromosomes, was first elucidated in 1988 by Moyzis et al.,[1] exactly a decade after the pioneering works from Blackburn and Gall on the *tetrahymena* telomeres.[2] The precise structure of the telomeric DNA is now known in detail:[3] it is comprised of hundreds of $[^{5'}TTAGGG^{3'}]/[^{3'}AATCCC^{5'}]$ repeats ended by a long (~200nt) single-stranded protrusion of the G-rich strand (termed 3′-overhang). This overhang is the focus of particular attention because G-rich DNAs are known to adopt a peculiar three-dimensional architecture, the G-quadruplex-DNA,[4] promoted by the formation of G-quartet, a coplanar association of four guanines through a precise Hoogsteen hydrogen-bonds pattern. A considerable wealth of knowledge has been acquired during the two last decades on the smallest model of the human telomeric G-quadruplex-DNA, the 24nt sequence $[TTAGGG]_4$ (and the closely related short quadruplex-forming sequences); in sharp contrast, little is known about the structure and function of longer telomeric sequences. It is intriguing because, over the past years, discrete quadruplexes have found applications mainly as anticancer targets,[5] but also as building blocks for nanodevices,[6] chiral auxiliary for stereoselective chemistry,[7] catalyst for oxidation reaction,[8] etc. This latter functionality deserves particular attention: it is indeed known from the pioneering investigations of Sen et al. that quadruplex-DNA may acquire enzyme-mimicking oxidative properties (related to peroxidases), upon interaction with hemin and H_2O_2 that respectively act as cofactor (activated upon binding to one of the accessible G-quartets of the quadruplex structure) and oxidizing agent.[9] This process, termed DNAzyme (schematically depicted in Figure 1A), found dozens of applications, including the detection of cations,[10] proteins,[11] nucleotides,[12] or cancer cells,[13] and has been exploited for the development of several biophysical assays[14] and DNA logic gates systems.[15] Interestingly, Willner and colleagues recently reported on a DNAzyme-based in vitro assay that enables the quantification of the telomerase activity.[16] This assay hinges on the 3′-overhang elongation by the human telomerase,[17] an enzyme whose existence has been firmly established in 1990 by Morin,[18] on the basis of pioneering works of Blackburn and Greider,[19] still on *tetrahymena*. The principle, schematically depicted in Figure 1B, thus relies on three highly interrelated hypotheses, the relationships between (1) telomerase activity and telomeric DNA length (the more active is the telomerase, the longer is the telomeric DNA), (2) telomeric length and quadruplex formation (the longer is the 3′-overhang, the more quadruplex units are formed), and (3) quadruplex formation and DNAzyme activity (the more quadruplexes are formed, the better is the DNAzyme activity). However, as above-mentioned, very

Received: August 29, 2011
Published: November 03, 2011

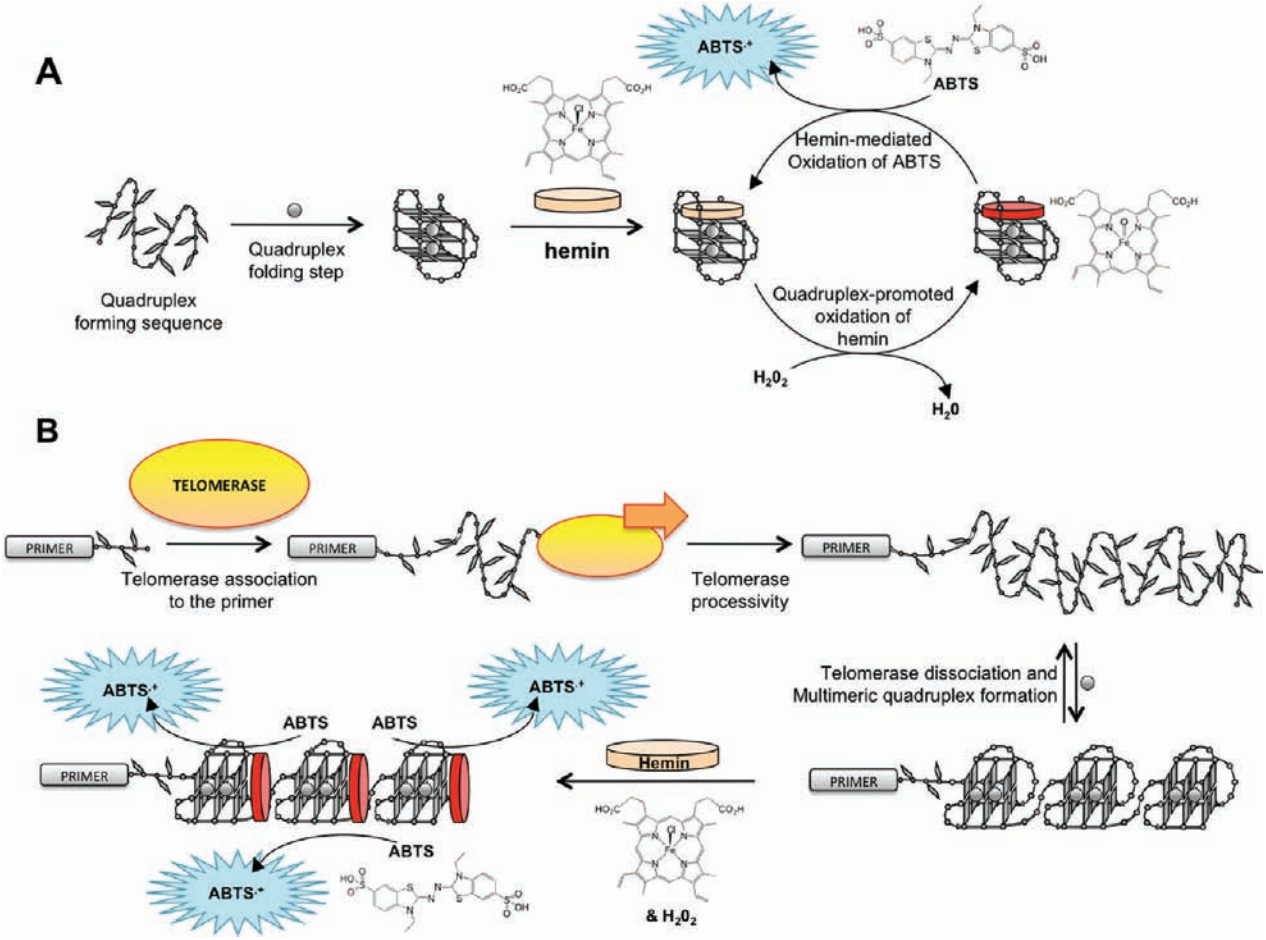

Figure 1. Schematic representation of the quadruplex-mediated DNAzyme process (A) and of the DNAzyme-mediated in vitro telomerase activity detection assay (B).

little is known about the structure (notably in terms of the putative formation of successive quadruplex units, known as multimeric quadruplexes) and function of longer telomeric sequences (notably their DNAzyme properties).[16c] This explains why considerable efforts are currently invested to decipher the actual shape and role of long telomeric sequences: given that they are comprised of numerous contiguous TTAGGG repeats, they can readily fold into several consecutive quadruplex units to adopt a so-called "beads-on-the-string" structure,[20] in which the quadruplex units are linked together through TTA linkers. This higher-order organization, probably of critical biological relevance, is, however, somewhat uneasy to characterize: an interesting impetus was given in 2006 by Sugimoto and co-workers,[20] via the study of long telomeric fragments through an array of biophysical assays (i.e., CD, UV−vis, and PAGE analyses), further substantied and explored in a recent study from Viglasky and co-workers.[21] Molecular modeling methods were subsequently used to build realistic models of mutimeric quadruplexes,[22] whose existence was firmly established in 2009 via atomic force measurement (AFM) investigations.[23] These results have prompted chemists to develop small molecules able to specifically interact with the quadruplex−quadruplex interface (or quadruplex interface), the junction region between two quadruplex units. The precise nature of this interface remains to be elucidated: on the basis of foregoing crystallographic investigations,[24] Neidle et al. proposed a model in which the interface is comprised of two fairly stacked G-quartets from two adjacent quadruplexes,[22a,c] thereby enabling the putative insertion (intercalation) of only one small molecule; alternatively, Chaires et al. have built a model in which the two quadruplex units are mostly independent,[22b,d] thereby allowing the possible fixation of more than one molecule. This particular binding site being thus characterized by unprecedented structural features that make its selective targeting feasible, it has offered chemical biologists possibilities for the design of innovative telomere targeting agents with a fully original higher-order DNA target. To date, two classes of compounds have been reported as quadruplex interface targeting agents;[25] interestingly, these studies have demonstrated that this interface is a highly hydrophobic cleft that displays a high affinity for small-molecules ligands and may accommodate, at best, one molecule at a time. These results are drastically important for the DNAzyme process because it has been demonstrated that a hydrophobic hemin-binding pocket leads to better DNAzyme results;[9] thus, it rapidly turned out that the quadruplex interface might be a site of high hemin-mediated DNAzyme activity. Herein, we report on the study of the DNAzyme activity of long telomeric sequences (and so, multimeric quadruplexes); our results not only substantiate the notion that lengthy telomeric stretches do not fold into a perfect beads-on-a-string higher-order organization, but also open

interesting perspectives to improve their DNAzyme activity (notably via the creation of artificial high-activity hemin-binding sites), with an eye toward finally improving the DNAzyme-based in vitro telomerase assay.

EXPERIMENTAL SECTION

UV−vis experiments carried out in 1 mL cuvette have been performed on a JASCO V630Bio spectrophotometer with a six-cell holder and 96-well plate experiments on a ThermoScientific Multiskan GO microplate spectrophotometer. DNA was purchased from Eurogentec (Belgium) in OligoGold purity grade at ∼200 nmol scale for 22AG (purified by RP-HPLC), at ∼1000 nmol scale for 46AG, 52AG, and 58AG (purified by IEX-HPLC), and at ∼1000 nmol scale for 70AG (purified by PAGE). Hemin was purchased from Sigma-Aldrich at 99% purity; DOTASQ (for DOTA-templated synthetic G-quartet) was synthesized according to previously reported procedures.[26]

Preparation of Oligonucleotides. DNAs were prepared by mixing 80 μL of DNA mother solution (500 μM in strands in deionized water (18.2 MΩ cm resistivity)), 16 μL of a 100 mM KCl/900 mM LiCl solution, 16 μL of a lithium cacodylate solution (100 mM, pH 7.2), and 48 μL of water. The final concentration of the prepared aliquots was theoretically 250 μM in 10 mM lithium cacodylate buffer (pH 7.2) + 10 mM KCl/90 mM LiCl; the actual concentrations DNA aliquots were evaluated via UV−vis spectra analysis at 260 nm, using the molar extinction coefficient value provided by the manufacturer. The higher-order structures of the DNAs were obtained by heating the solutions at 90 °C for 5 min, cooling in ice for 6 h to favor the intramolecular folding, and then were stored at least overnight at 4 °C.

DNAzyme Experiments. All of the experiments were carried out with Caco·KTD buffer,[27] comprised of 10 mM lithium cacodylate buffer (pH 7.2) plus 10 mM KCl/90 mM LiCl, 0.05% Triton X-100, and 0.1% DMSO. Mother solutions were ABTS (20 mM in water), hemin (1 mM in Caco.KTD for 1 mL cuvette experiments or 0.1 mM in DMSO for 96-well plate experiments), DNA aliquots (250 μM, vide supra), H_2O_2 (60 mM in water), and DOTASQ (1 mM in a 9/1 water/DMSO solution). The 1 mL cuvette experiments (performed at 25 °C) were carried out with 2 mM ABTS, 1 μM hemin, 0.6 mM H_2O_2, and variable amounts of both DNA and DOTASQ, depending on the conditions: for experiments carried out (a) at 1:1 hemin:DNA strand ratio, 885 μL of Caco·KTD plus 1 μL of hemin and 4 μL of DNA aliquot; (b) at 1:1 hemin:quadruplex unit ratio, 885 μL of Caco·KTD plus 1 μL of hemin and 4 μL of 22AG, or 887 μL of Caco·KTD plus 1 μL of hemin and 2 μL of 46AG, or 887.7 μL of Caco·KTD plus 1 μL of hemin and 1.33 μL of 70AG; (c) at 1:1 hemin high-activity site ratio, 885 μL of Caco·KTD plus 1 μL of hemin and 4 μL of 46AG, or 887 μL of Caco·KTD plus 1 μL of hemin and 2 μL of 70AG; (d) with DOTASQ, Caco·KTD (from 825 to 885 μL) plus DOTASQ (from 0 to 60 μL) and 1 μL of hemin and 4 μL of DNA aliquots; and (e) for control ("background") experiments, 889 μL of Caco·KTD plus 1 μL of hemin. The experiments performed at higher hemin doses (2 and 3 μM) were carried out with 2 mM ABTS, 0.6 mM H_2O_2, and variable amounts of both hemin and DNA, depending on the conditions: (a) two 22AG versus one 46AG, 880 μL of Caco·KTD plus 2 μL of hemin and 8 μL of 22AG versus 884 μL of Caco·KTD plus 2 μL of hemin and 4 μL of 46AG; and (b) three 22AG versus one 70AG, 875 μL of Caco·KTD plus 3 μL of hemin and 12 μL of 22AG versus 883 μL of Caco·KTD plus 3 μL of hemin and 4 μL of 70AG. The mixtures were stirred at room temperature for 45 min, and then 100 μL of ABTS was added, and the DNAzyme reactions were launched by the addition of 10 μL of H_2O_2. The 96-well plate experiments (performed at 25 °C) were carried out with 2 mM ABTS, 1 μM hemin, 0.6 mM H_2O_2, and variable amounts of DNA (from 8 to 0.065 μM), in the absence or presence of DOTASQ (50 μM), depending on the conditions: (a) two mother solutions (at 250 and 25 μM) were prepared for each DNA, which corresponds to an addition of 3.2, 1.6, 0.8, and 0.4 μL (of the solution at 250 μM), then 2.0, 1.0, 0.5, and 0.25 μL (of the solution at 25 μM) on a sufficient quantity of Caco·KTD buffer for 89 μL final volume for experiments carried out without DOTASQ or 84 μL final volume for experiments carried out with 5 μL of DOTASQ in each well; (b) for DOTASQ-free control experiments, 88 μL of Caco·KTD plus 1 μL of hemin; and (c) for DOTASQ control experiments, 83 μL of Caco·KTD plus 1 μL of hemin and 5 μL of DOTASQ. The mixtures were stirred at room temperature for 45 min, and then 10 μL of ABTS was added and the DNAzyme reactions were launched by the addition of 1 μL of H_2O_2.

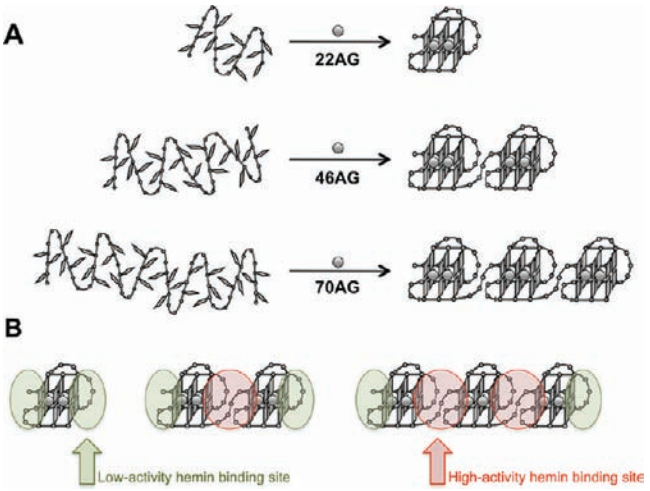

Figure 2. Schematic representation of 22AG, 46AG, and 70AG (random coiled and folded structures, A) and their putative low-activity (green) or high-activity (red) hemin-binding sites (B).

Data Treatment. The characteristic UV−vis signal (Abs@420 nm) of $ABTS^{\cdot+}$ was plotted as a function of time (min) with OriginPro8 software (OriginLab Corp. Northampton, MA); raw data of experiments were subtracted from the control experiment (to obtain the "specific" DNAzyme activity) and zeroed at their initial point. For V_0 determination, the Abs@420 nm at the very first four points was plotted as a function of time and linearly fitted to access the slope of this linear function, which corresponds to V_0 (in Abs min^{-1}) subsequently converted in μM min^{-1} via the Beer−Lambert law: Abs = $\varepsilon \cdot l \cdot c$, with $\varepsilon(ABTS^{\cdot+})$ = 36 000 M^{-1} cm^{-1}.

RESULTS AND DISCUSSION

DNAzyme Activities of 22AG, 46AG, and 70AG: Implications in Terms of Hemin-Binding Sites. To decipher the actual DNAzyme activity of multimeric quadruplexes, we decided to study telomere-mimicking fragments of three different lengths, 22AG ($AG_3(T_2AG_3)_3$), 46AG ($AG_3(T_2AG_3)_7$), and 70AG ($AG_3(T_2AG_3)_{11}$), respectively, comprised of 4, 8, and 12 telomeric repeats. These sequences can consequently fold into a single, two, or three quadruplex units (Figure 2A); however, contrary to 22AG,[4] the folding state of longer telomeric fragments has been poorly investigated.[21] To assess these higher-order structures, TDS (thermal differential spectra) measurements were first performed:[28] as depicted in the Supporting Information (Figure S1), the three sequences display a TDS signature that is typical, and thus strongly indicative, of a quadruplex (for 22AG) or a quadruplex-based higher-order (for 46AG and 70AG) architecture. To gain further insight into their detailed structures (notably in terms of the nature of the quadruplex

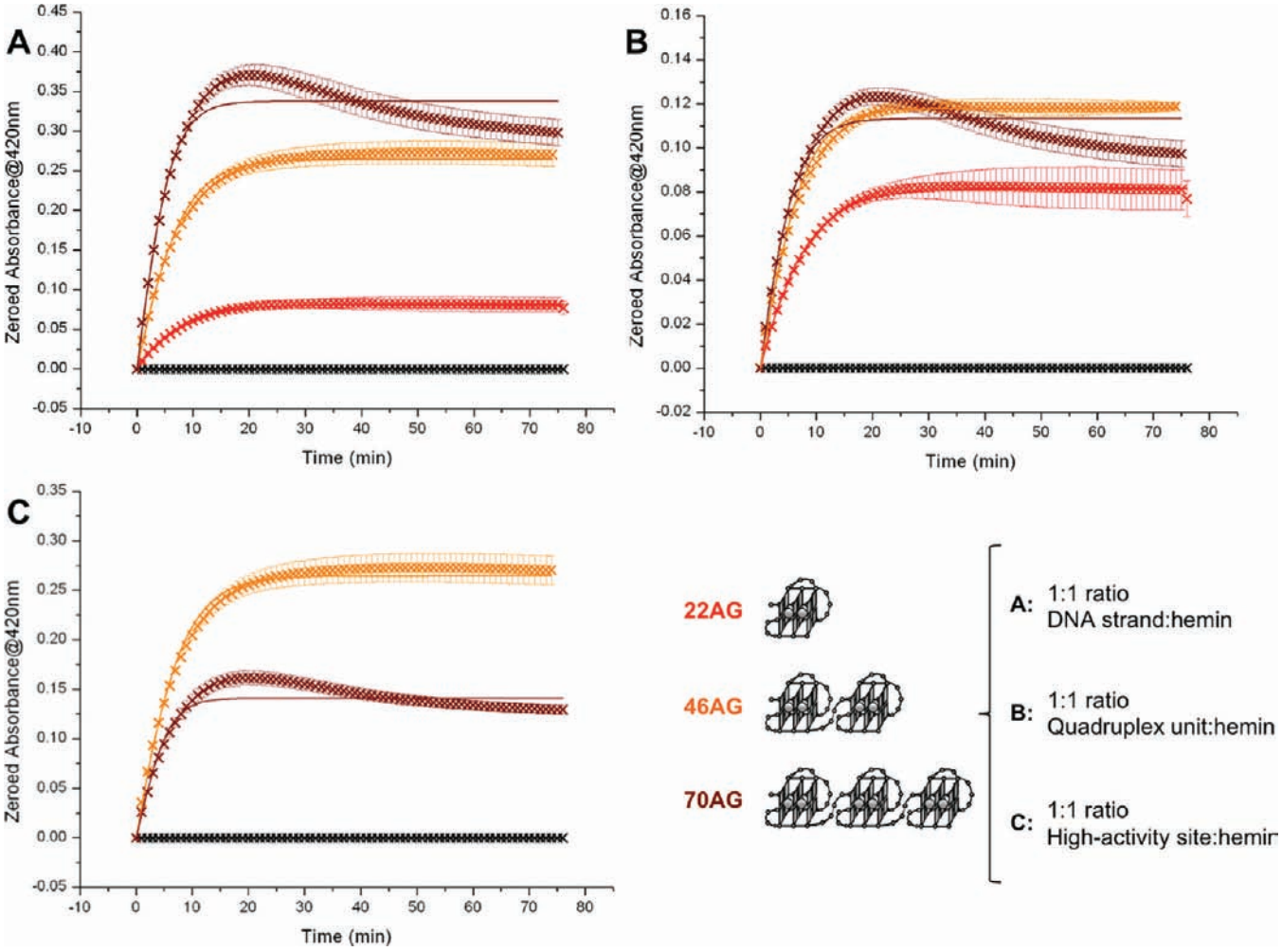

Figure 3. Compared DNAzyme activity of experiments carried out with hemin (1 μM), H_2O_2 (0.6 mM), and ABTS (2 mM) in the absence of DNA (black line) or with 22AG (red line, 1 μM A/B), 46AG (orange line, 1 μM A/C, 0.50 μM B), and 70AG (brown line, 1 μM A, 0.33 μM B, 0.50 μM C) in Caco·KTD buffer, pH 7.2 at 25 °C.

folding (i.e., the so-called parallel, antiparallel, and hybrid-type foldings)),[4] CD (circular dichroism) analyses were subsequently carried out: while we recognize the necessity to be cautious in drawing too firm structural conclusions solely from CD signatures,[29] obtained CD spectra (see Figure S2, Supporting Information) agree with a hybrid-type quadruplex structure for 22AG, and lend credence to the model proposed by Komiyama[23] and Yang[30] of a succession of hybrid-type quadruplexes for 46AG and 70AG (as represented in Figure 2A).

We thus performed a first series of DNAzyme experiments with 22AG, 46AG, and 70AG as DNA matrices, ABTS (2,2′-azinobis(3-ethylbenzothiazoline)-6-sulfonic acid) as a reporter probe, according to our previously reported protocol (i.e., 2 mM ABTS and 1 μM hemin in Caco·KTD buffer (i.e., 10 mM lithium cacodylate buffer (pH 7.2) plus 10 mM KCl/90 mM LiCl, 0.05% Triton X-100 and 0.1% DMSO), the reaction being initiated by the addition of 0.6 mM H_2O_2);[27] of note, we used herein 1 μM DNA (expressed in strand concentration) instead of the 2 μM DNA initially used,[27] because it has been recently shown that the most oxidatively active assembly is comprised of a 1:1 DNA:hemin association.[31] The reaction is conveniently monitored via the appearance of a UV−vis signal at 420 nm, characteristic of the $ABTS^{\cdot+}$ product.[9] As depicted in Figure 3A, the three DNA/hemin systems were found active to oxidize ABTS; interestingly, despite a similar concentration of hemin (1 μM), that is, a similar bound hemin/DNA ratio, the peroxidatic activity of the DNAs is not equivalent: 70AG is indeed found better than 46AG, itself far better than 22AG. To valuably compare these peroxidatic activities, we quantify them via their initial velocity (V_0, expressed in μM min^{-1}),[27] defined as the concentration of $ABTS^{\cdot+}$ synthesized at the very beginning of the reaction as a function of time: herein, V_0 = 0.27, 0.93, and 1.51 μM min^{-1} for 22AG, 46AG, and 70AG systems, respectively (see the Supporting Information).

These differences of catalytic behavior are strongly indicative of a difference of hemin-binding site within the three DNA architectures. Indeed, two different types of hemin-binding pocket can be defined, hereafter termed "external" (i.e., between an external quartet and a surrounding loop (highlighted in green, Figure 2B)) and "internal" binding sites (i.e., at the quadruplex interface, in red in Figure 2B). By nature, these two types of hemin-binding sites greatly differ because the hemin within an external binding site will be less protected against external medium (more solvent-accessible) and in a less hydrophobic environment than within an internal site. These observations may greatly impact the hemin-related catalytic activity of the hemin/DNA complexes because

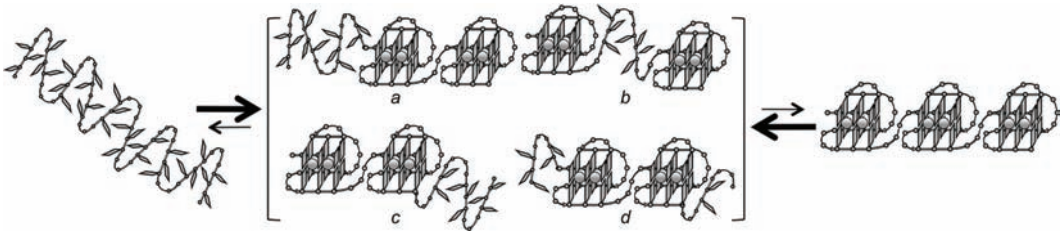

Figure 4. Schematic representation of the probable conformational plurality of 70AG (see text for a−d explanations).

Sen et al. have clearly demonstrated that these two factors (protection against H_2O_2-degradation and hydrophobicity of the binding site) greatly enhance the catalytic rate of the system.[9] Therefore, it is expected that a hemin bound within an internal site will be more oxidatively active than a hemin bound within an external site. As depicted in Figure 2B, 22AG, 46AG, and 70AG are thus nonequivalent in terms of binding sites because 22AG has two external sites (or presumably "low-activity hemin-binding sites"), 46AG has two external sites and one internal site (or presumably "high-activity hemin-binding site"), and 70AG has two external and two internal sites: these differences may account for the higher activity of 70AG as compared to 46AG, which is itself more active than 22AG.

To further investigate this high-activity site dependency, three other series of DNAzyme experiments (with fixed hemin concentrations, to have, in each case, similar background reactions) were performed.

(1) To first rule out an explanation solely based on the number of constitutive quadruplex units, DNAzyme experiments were performed at 1:1 quadruplex unit:hemin ratio (i.e., a 1:1, 0.5:1, and 0.33:1 DNA:hemin ratio for 22AG, 46AG, and 70AG, respectively, the concentration of hemin being fixed at 1 μM): as depicted in Figure 3B, the performances of the DNAs are not similar, thereby demonstrating that their activities do not depend on the number of the constitutive quadruplex units. The better performance of 46AG as compared to 22AG (1.6-fold more active, V_0 = 0.43 and 0.27 μM min^{-1}, respectively; see the Supporting Information) indicates that the peroxidatic activity of the resulting system depends on the presence of high-activity hemin-binding sites. The low difference between 46AG and 70AG (V_0 = 0.43 and 0.48 μM min^{-1}, respectively) is interesting because it additionally indicates that, while the former very probably adopts mainly a two-quadruplex higher-order structure, the latter may exist as an equilibrium of different multimeric structures, mainly with two simultaneously folded quadruplexes, reminiscently of what has been reported recently by Viglasky et al. (Figure 4).[21]

(2) To assess the actual impact of the high-activity site, DNAzyme experiments were subsequently performed at 1:1 high-activity site:hemin ratio (i.e., a 1:1 and 0.5:1 DNA:hemin ratio for 46AG and 70AG, respectively, the concentration of hemin being fixed at 1 μM, 22AG being not evaluated because it does not display high-activity site): the lower activity of 70AG as compared to 46AG (V_0 = 0.63 and 0.93 μM min^{-1}, respectively; see the Supporting Information) again supports that 70AG probably does not elicit two high-activity sites concomitantly, thus inferring that it may probably exist as an equilibrium of different multimeric structures rather than as a three-quadruplex structure (Figure 4).

(3) To firmly establish the role played by the high-activity sites, comparative DNAzyme experiments were finally performed, again at 1:1 quadruplex unit:hemin ratio (vide supra) but at fixed and higher hemin concentrations (i.e., in the first series, the efficiency of a system comprised of 22AG:hemin at 2:2 ratio is compared to that of a system comprised of 46AG:hemin at 1:2 ratio; in the second series, the efficiency of a system comprised of 22AG: hemin at 3:3 ratio is compared to that of a system comprised of 70AG:hemin at 1:3 ratio): as depicted in Figure 5, the better performance of one 46AG (V_0 = 1.14 μM min^{-1}) as compared to two 22AG (V_0 = 0.74 μM min^{-1}) clearly highlights the positive impact of the presence of one high-activity site within the 46AG structure; similarly, the better performance of one 70AG (V_0 = 2.63 μM min^{-1}) as compared to three 22AG (V_0 = 1.80 μM min^{-1}) again highlights the positive impact of the presence of two high-activity sites within the 70AG structure.

Altogether, these results not only concur in demonstrating that long telomeric fragments do not necessarily fold into perfect higher-order stacked-quadruplex structures, but also strongly demonstrate the significant influence of the hydrophobicity of the hemin-binding site (external vs internal) on the DNAzyme process. To further investigate this, it was of interest to study the catalytic properties of telomeric fragments longer than 46AG but shorter than 70AG, that is, able to fold into two-quadruplex architectures with a higher degree of flexibility (notably around the interface). Two candidates, 52AG ($AG_3(T_2AG_3)_8$) and 58AG ($AG_3(T_2AG_3)_9$), were used as DNAzyme catalysts; the logic behind using these sequences is to offer the oligonucleotides the possibility of adopting a structure in which two quadruplex units are connected through longer linkers (up to 9 and 15 nucleotides for 52AG and 58AG, respectively, vs 3 for 46AG), but unable to form a three-quadruplex architecture (unlike 70AG). This flexibility may be valuable for improving the interaction with hemin, putatively enabling a better induced fit mechanism during the hemin/DNA association. As depicted in the Supporting Information (Figure S3), the catalytic activities of 52AG and 58AG were found intermediate (V_0 = 1.06 μM min^{-1} for both 52AG and 58AG) between that of 46AG (V_0 = 0.79 μM min^{-1}) and 70AG (V_0 = 1.42 μM min^{-1}). These results thus enlighten not only the positive contribution of the flexibility around the interface, but also its own limit because identical V_0 values were obtained with 52AG and 58AG, thereby inferring that the 9-nucleotide linker of 52AG may provide an optimal flexibility. This series of experiments consequently enables one to gain valuable insights into the 70AG-related oxidatic mechanism: the better activity of 70AG as compared to 52AG indicates that 70AG does not solely adopt a two-quadruplex architecture in which the units are connected by a long linker (from 3 up to 27-nucleotide; given that 52AG and 58AG are equally efficient, 70AG would have been also equally active as 52AG); this observation implies that an additional contribution takes place only with 70AG, likely related to its unique ability to fold into a three-quadruplex higher-order structure, and so to offer a transient formation of two high-activity sites within its structure.

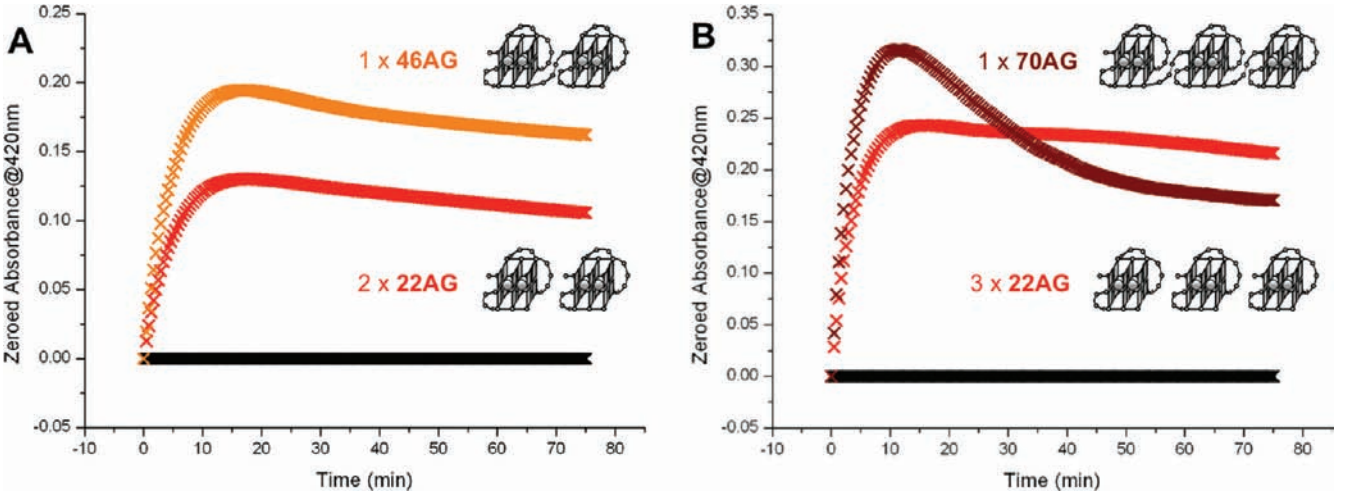

Figure 5. Compared DNAzyme activity of experiments carried out with H_2O_2 (0.6 mM), ABTS (2 mM), and (A) 2 μM hemin in the absence of DNA (black line) or with 2 μM 22AG (red line) versus 1 μM 46AG (orange line); (B) 3 μM hemin in the absence of DNA (black line) or with 3 μM 22AG (red line) versus 1 μM 70AG (brown line), in Caco·KTD buffer, pH 7.2 at 25 °C.

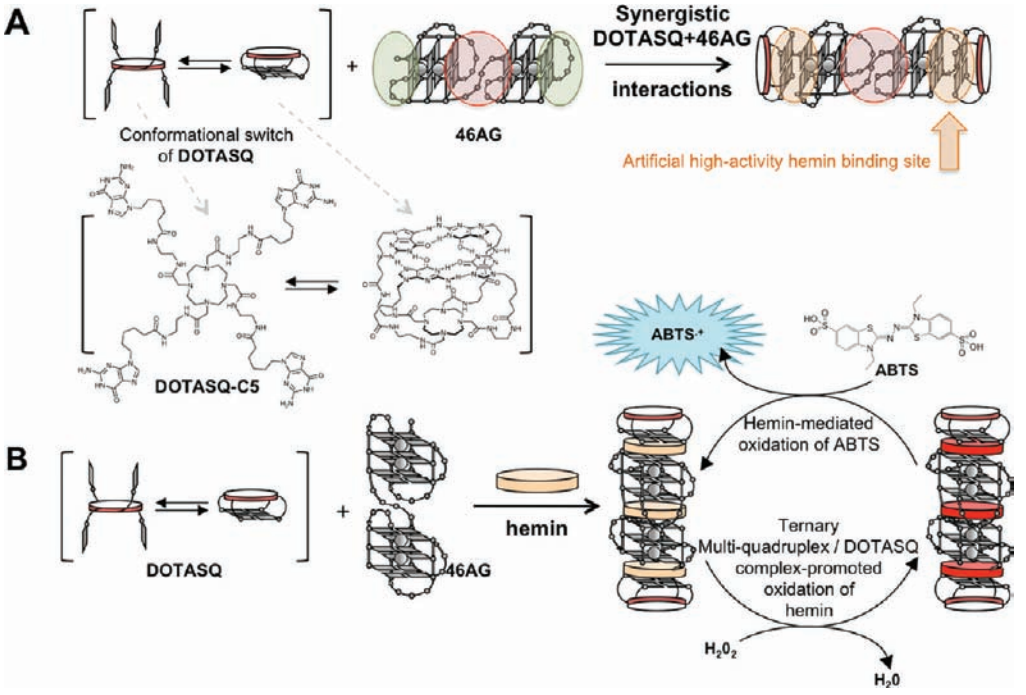

Figure 6. (A) Schematic representation of the conformational switch of DOTASQ (left panel) and the creation of an artifical high-activity hemin-binding site (highlighted in orange) upon synergistic interaction between DOTASQ and 46AG (right panel). (B) Schematic representation of the multimeric quadruplex-mediated DNAzyme process boosted by the presence of DOTASQ.

Improving the DNAzyme Activity of Multimeric Quadruplexes via the Creation of an Artificial High-Activity Hemin-Binding Site. On the basis of the aforementioned conclusions, we reasoned that a way to improve the overall catalytic activities of 22AG, 46AG, and 70AG may be to artificially recreate the hydrophobic conditions of an internal binding site at an external site: this can be achieved, for example, by sandwiching hemin between the external quartet of the DNA and an artificial G-quartet. To this end, we employed the small-molecule DOTASQ (for DOTA-templated Synthetic G-Quartet)[26,27] whose structure is conformationally labile (i.e., DOTASQ adopts an "open" and a "closed" conformation in solution, Figure 6A). The intramolecular G-quartet fold of DOTASQ makes it able to interact both with quadruplex-DNA (thereby behaving as a G-quadruplex ligand that interacts with its target according to a biomimetic approach)[26] and small molecules, particularly the negatively charged porphyrins (including hemin): this latter observation has led to the use of DOTASQ as catalyst for a DNAzyme-like process,[27] which revealed to be yet effective but admittedly modest as compared to quadruplex catalytic activities (it was nevertheless the first demonstration that an isolated and fully synthetic G-quartet may catalyze an hemin-mediated oxidation

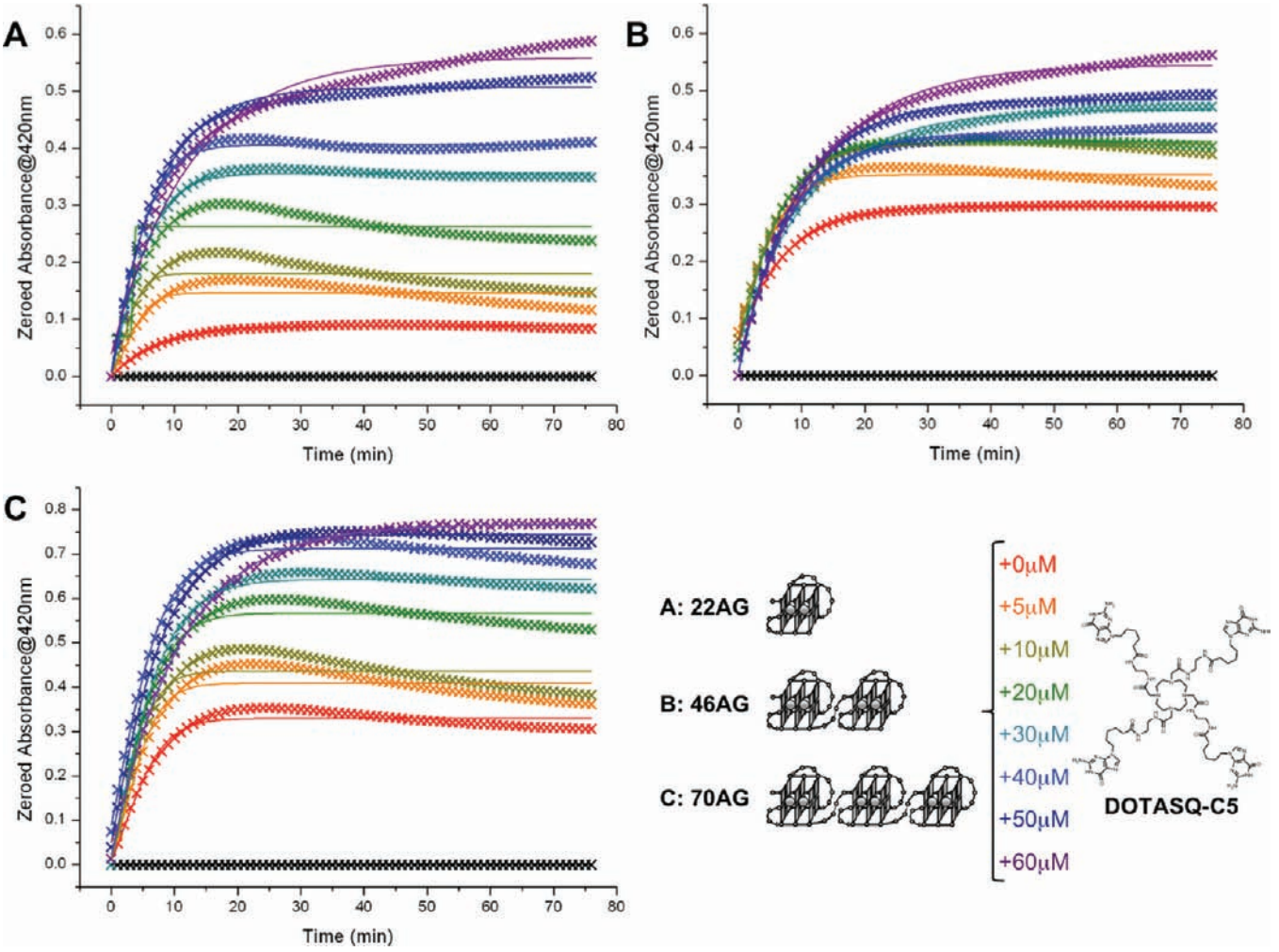

Figure 7. Compared DNAzyme activity of experiments carried out with hemin (1 μM), H_2O_2 (0.6 mM), and ABTS (2 mM) in the absence of DNA (black lines) or with 1 μM 22AG (A), 46AG (B), and 70AG (C) without (red lines) or with DOTASQ (from 5 (orange lines) to 60 μM (purple lines)) in Caco·KTD buffer, pH 7.2 at 25 °C.

process). We thus reasoned that DNA and DOTASQ may concomitantly interact with hemin ("sandwiching" it, as is schematically described in Figure 6), thereby synergistically interacting to provide a DNA/DOTASQ adduct with only high-activity hemin-binding sites (i.e., high-activity hemin-binding site and "artificial high-activity hemin-binding site", in red and orange, respectively, in Figure 6A). Nevertheless, using concomitantly DNA (at 1 μM dose) and DOTASQ (in excess, up to 60 μM dose, vide infra) may raise several conflicting situations that need to be taken into account:

(1) A competition can take place between DOTASQ and hemin for the quadruplex binding site: DOTASQ has been indeed demonstrated to be a weak G-quadruplex ligand,[26] but in a low ligand-to-quadruplex ratio (5:1); when DOTASQ is used at higher doses, its quadruplex-binding properties are clearly enhanced (with $\Delta T_{1/2}$ values from 1.7 (5:1 ratio) up to 6.6 °C (25:1 ratio), monitored by FRET-melting experiments (see Figure S4, Supporting Information)).[32] Thus, at high concentrations, DOTASQ may sequester the DNA under a DOTASQ/DNA complex, thereby inhibiting its DNAzyme activity. This may result in a DNAzyme activity relying only on remaining DOTASQ in solution, that is, in an unmodified DNAzyme activity as compared to DOTASQ alone. (2) The hemin can be randomly distributed between DOTASQ and DNA, thus resulting in a final DNAzyme activity comprised between that of DNA alone and DOTASQ alone. (3) The hemin can bind alternatively DOTASQ and DNA, thus resulting in a final DNAzyme activity that corresponds to the addition of the activities of both DOTASQ and DNA alone. (4) Finally, a synergistic cooperation can take place between the DNA and the DOTASQ, which may originate in the concomitant hemin π-stacking by both partners, thus creating an unprecedented sandwich interaction closely related to an artificial hemin intercalation between two G-quartets, one from the quadruplex and the other from DOTASQ (Figure 6).

We first investigated the peroxidatic activity of DOTASQ on a broader concentration range (from 0 to 100 μM) than previously reported (0−50 μM);[27] as depicted in the Supporting Information (Figure S5), the catalytic efficiency of DOTASQ increases with its concentration up to a certain point, the optimum activity being reached with 60 μM DOTASQ. We thus decided to investigate the influence of the concomitant presence of DNA (1 μM 22AG, 46AG, and 70AG) and DOTASQ (from 0 to 60 μM) on the peroxidatic activity of the resulting systems

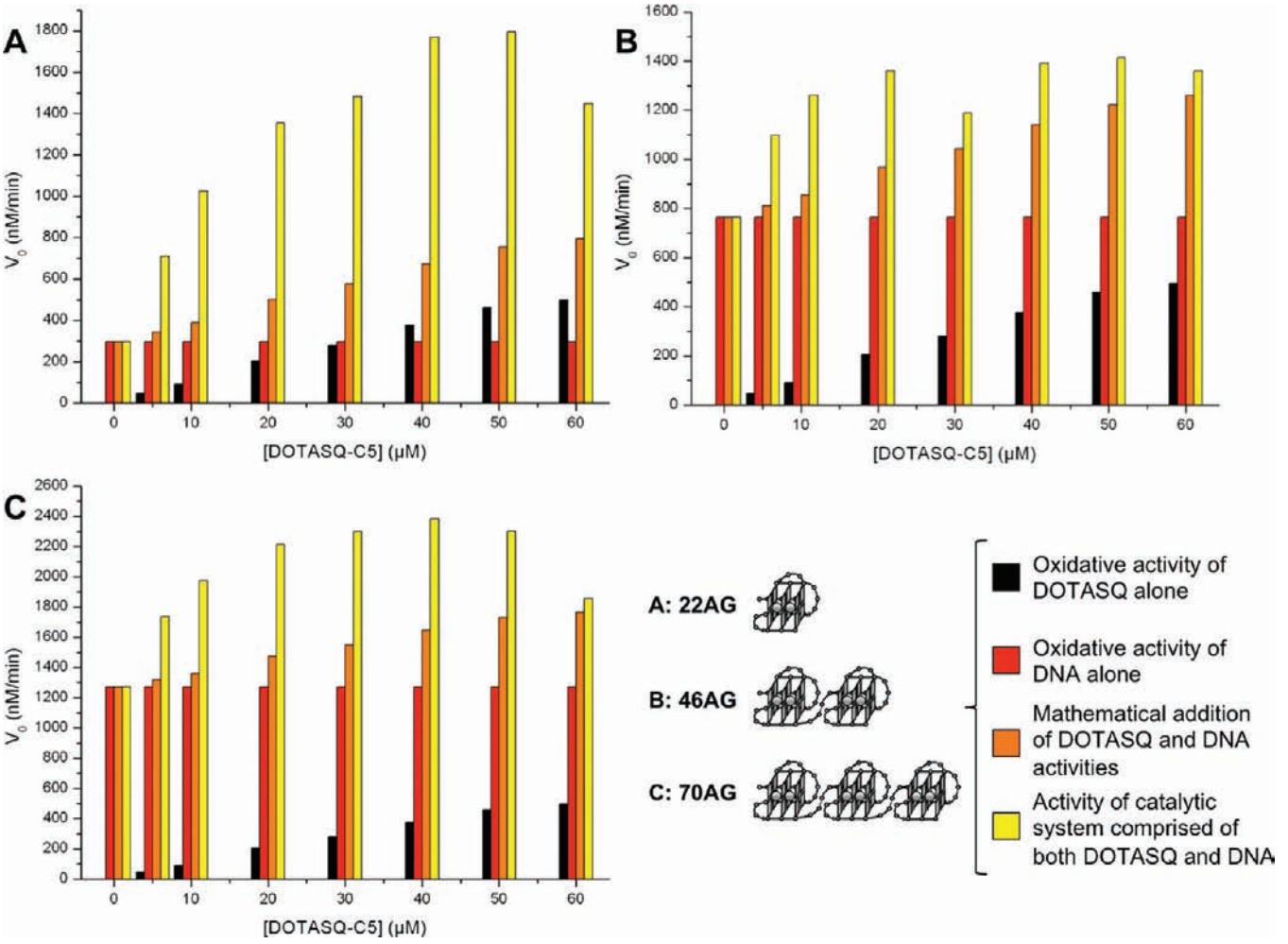

Figure 8. Diagrammatic bar representation of DNAzyme results (V_0 values) for experiments carried out with hemin (1 μM), H_2O_2 (0.6 mM), and ABTS (2 mM) with DOTASQ alone (from 0 to 60 μM, black bars), DNA alone (1 μM, red bars), or in the presence of both DNA (1 μM) and DOTASQ (from 0 to 60 μM) (yellow bars) in Caco·KTD buffer, pH 7.2 at 25 °C. The mathematical additions of the contributions of both DOTASQ and DNA alone are shown as orange bars.

(hereafter named "[DOTASQ+DNA] system"): as depicted in Figure 7, the presence of DOTASQ clearly enhances the DNAzyme properties of the DNAs (experiments performed at 1:1 DNA strand:hemin ratio). Indeed, in all cases, the catalytic activity of the [DOTASQ+DNA] systems is higher than that of the DNA alone (red curve, Figure 7). This series of results thus enables us to discard the hypotheses (1) competition and (2) distribution (vide supra) because, particularly for low DOTASQ doses, the resulting activities are always superior to that of the DNA alone. It was thus of high interest to find a way by which to settle on one of the two left hypotheses (i.e., (3) additive effect and (4) synergy (vide supra)): to this end, we decided to compare the V_0 values for experiments carried out with DOTASQ alone, DNA alone, and with the [DOTASQ+DNA] system (Figure 8 and Supporting Information). For sake of clarity, we concomitantly indicate the V_0 values of DOTASQ alone (black bars, Figure 8), DNA alone (red bars, Figure 8), the mathematical additions of the V_0 values of both DOTASQ and DNA alone (orange bars, Figure 8), and the V_0 values obtained for experiments carried out with the [DOTASQ+DNA] system (yellow bars, Figure 8). In all cases, the catalytic efficiency of the [DOTASQ+DNA] system is far beyond the mathematical addition of both contributions: these results testify to the synergistic cooperation that takes place between DNA and DOTASQ, probably via the creation of an artificial hemin intercalation site (schematically represented in Figure 6B), thereby enthroning the hypothesis (4) synergy as the experimentally validated one. Interestingly, the gain in efficiency is more pronounced for 22AG (up to 2.7-fold as compared to the mathematical addition of both contributions; see the Supporting Information) than for 46AG and 70AG (up to 1.5-fold); this can be readily rationalized because 22AG is initially devoid of any high-activity binding site and consequently more sensitive to the creation of such a high-activity site. Additionally, the observation that the effect is more pronounced for 70AG as compared to 46AG (the average gain being 1.36 vs 1.25-fold) is again in favor of a more important conformational plurality of 70AG as compared to 46AG; indeed, as depicted in Figure 4, 70AG may fold into various higher-order structures among which some of them may be comprised of two stacked quadruplex units (probably the favored situation, cases a, c,d in Figure 4) and some others comprised of two pseudoindependent discrete quadruplex units (case b, Figure 4), thereby behaving like 22AG (i.e., being sensitive to the creation of high-activity sites). Finally, the observation of relative loss of synergy

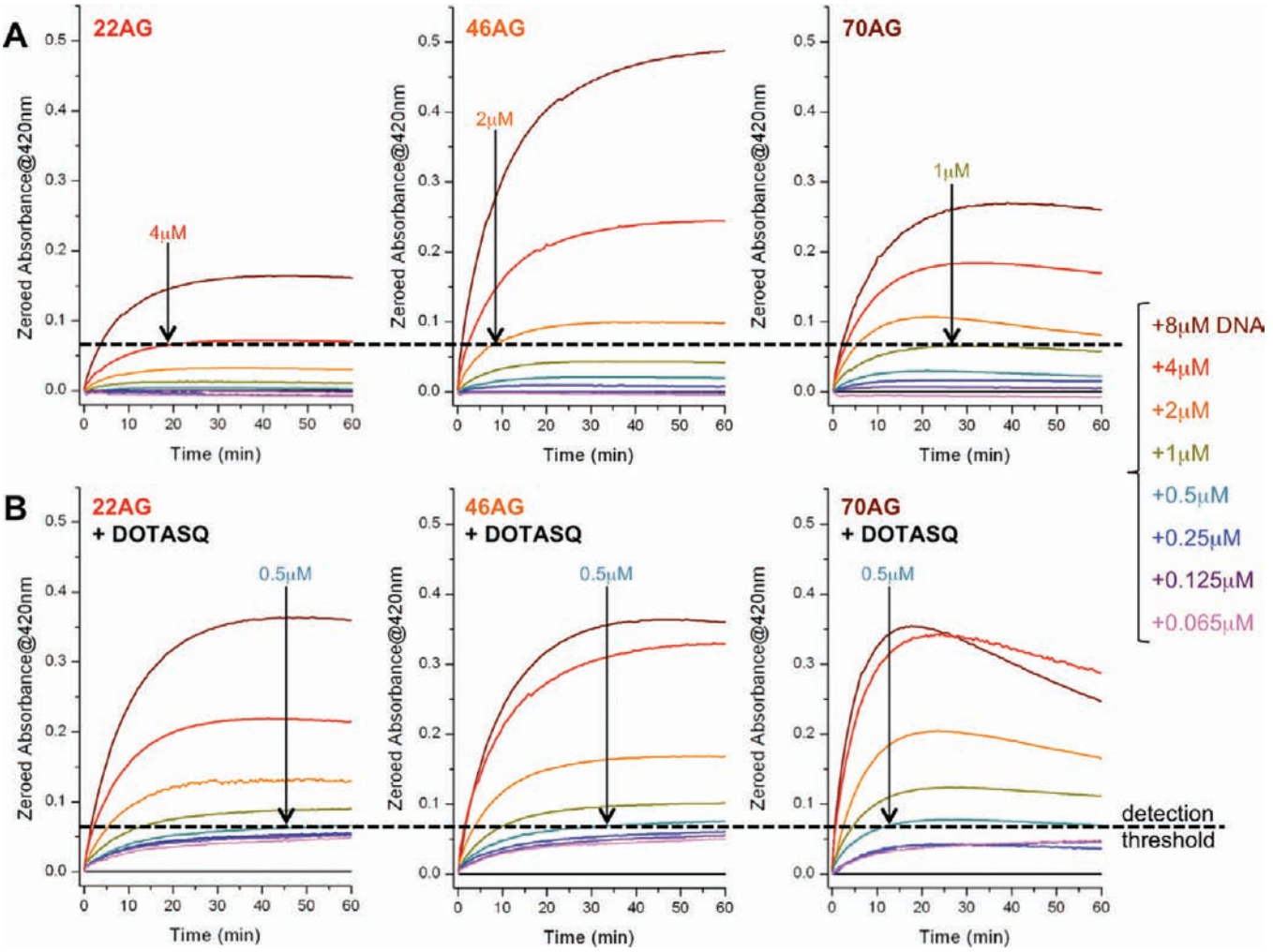

Figure 9. Compared DNAzyme activity of a 96-well plate experiment carried out with hemin (1 μM), H_2O_2 (0.6 mM), and ABTS (2 mM) in the absence of DNA (black lines) or with various DNA concentrations (from 8 μM to 65 nM), without (A) or with DOTASQ (B, 50 μM) in Caco·KTD buffer, pH 7.2 at 25 °C.

at the highest DOTASQ dose (60 μM) may indicate that using too high DOTASQ concentrations may be detrimental for the synergy by blurring the DOTASQ effect (increasing, for example, the contribution of the hypothesis (1) competition (vide supra)). Last, to gain further confidence into the synergistically proficiency of DOTASQ, we varied the experimental conditions, virtually saturating, for instance, the hemin-binding sites of the DOTASQ/DNA assemblies (i.e., 0.5:1, 0.33:1, and 0.25:1 DNA strand:hemin ratio for 22AG, 46AG, and 70AG, respectively) to be relevant to the model proposed in Figure 6B. As depicted in the Supporting Information (Figure S6), under these unoptimized conditions (far from the ideal 1:1 DNA strand:hemin complex displaying optimal oxidatic activity, vide supra),[31] further credence has been lent to this hypothesis by the observation that DOTASQ indeed interacts synergistically with DNA to promote enhanced DNAzyme experiments, even under saturating hemin concentrations. This observation is particularly important in light of the ultimate goal pursued, that is, the detection of low DNA quantities that result from their de novo synthesis by the telomerase.

To investigate this, a preliminary 96-well plate DNAzyme experiment was performed, also to further figure out the impact of the finding that the DNAzyme activity of quadruplex-forming oligonucleotides can be boosted by the addition of an artificial G-quartet (via the formation of an unprecedented ternary noncovalent catalytic system) on the detection threshold of this technique in the telomerase assay conditions. The experiment was carried out with decreasing concentrations (from 8 μM to 65 nM) of multimeric quadruplex-forming DNA (22AG, 46AG, and 70AG) in the absence or presence of DOTASQ as a molecular enhancer (50 μM): as depicted in Figure 9, in the microplate conditions, the $ABTS^{\bullet+}$ UV−vis signal ranges from 0 to 0.5; we thus arbitrarily fixed a "detection threshold" at 0.06, which corresponds to a signal that is 20% higher than that of the DOTASQ control experiments (i.e., carried out with DOTASQ alone), which levels off at 0.05 (see Figure S7, Supporting Information). So, each well in which the UV−vis response is >0.06 corresponds to a catalytic system active enough to produce significant and reliably detectable amounts of $ABTS^{\bullet+}$ product. As depicted in Figure 9, the detection threshold is reached with 4, 2, and 1 μM DNA (for 22AG, 46AG, and 70AG, respectively) in the unboosted experiments, while it is reached with 0.5 μM DNA in the three boosted experiments. This enlightens the positive contribution of DOTASQ as an enhancing element, because it increases by a factor up to 8-fold the sensitivity of the detection

dx.doi.org/10.1021/ja208145d |J. Am. Chem. Soc. 2011, 133, 20405–20415

of the method. A possibility to further improve this sensitivity, to ultimately make a limit of quantification in the low nanomolar range possible, relies on a fine-tuning of the DOTASQ concentration (along with that of the other reactants) for the microplate experiments; we are currently investing efforts in these optimizations and hope to report on this soon.

CONCLUSIONS

We report herein on an unprecedented investigation aiming at deciphering the DNAzyme activity of long telomeric fragments. The interpretation of the present array of results can be 3-fold: from the DNA point of view, the present study tends to demonstrate that long telomeric sequences indeed adopt multimeric quadruplex folds, but not in a direct and linear relationship with their lengths. They also shed light on the fact that fragments with even numbers of quadruplex units may display not only a more stable higher-order fold (originating in intramolecular quadruplexes stacks) but also an optimized three-dimensional organization for promoting DNAzyme experiments (thanks to the existence of a naturally occurring high-activity hemin-binding site at the quadruplex interface). Longer telomeric fragments (like 94AG $(AG_3(T_2AG_3)_{15})$ or 118AG $(AG_3(T_2AG_3)_{19})$) have thus to be synthesized and studied in the aim of ascertaining if this observation can be extended and generalized to very long telomeric fragments. From the DOTASQ point of view, the present study clearly highlights the versatility of this molecular tool: DOTASQ has been indeed previously reported as a G-quadruplex ligand,[26] and precatalyst for a quadruplex-free DNAzyme process,[27] and herein its scope is extended because it acts as a "boosting agent" of quadruplex-mediated DNAzyme experiments. This study thus keeps on demonstrating that artificial G-quartets are highly valuable molecular tools, thereby underlining that efforts are to be undertaken to develop new generations of water-soluble TASQ (for template-assembled synthetic G-quartet)[33] compounds displaying a highly stable G-quartet fold. Finally, from the telomerase assay point of view, the present study first offers a way to improve the sensitivity of the method (up to 8-fold) via the addition of a molecular enhancer (herein DOTASQ). Second, this study points out that, because the relationship between telomere length and DNAzyme activity is not direct, caution has to be exercised in interpreting the results; to gain further confidence in this assay, it may thus be highly valuable to add an extra experimental step in the telomerization methodology reported by Willner et al. (i.e., (1) telomerase-mediated primer extension, (2) quadruplex-folding and hemin association, and (3) DNAzyme-based optical analysis),[16] in which an endonuclease-mediated partial digestion step of the freshly synthesized telomeric fragment is performed to obtain short fragments (ideally of 46AG length) that will adopt a higher-order conformation optimal for performing efficient DNAzyme reactions.

The time is thus ripe for us to play with cell lysates, telomerase extracts, and endonucleases; we hope to report on these investigations in the near future.

ASSOCIATED CONTENT

Supporting Information. Additional CD, TDS, FRET-melting, and DNAzyme experiments, and tables summarizing all calculated V_0 values. This material is available free of charge via the Internet at http://pubs.acs.org.

AUTHOR INFORMATION

Corresponding Author
david.monchaud@u-bourgogne.fr

ACKNOWLEDGMENT

We thank A. Guédin and J.-L. Mergny for the FRET-melting experiments and fruitful discussions, F. Cuenot for project help, CheMatech company for assistance with the DOTASQ synthesis, and the CNRS, the Université de Bourgogne, the Conseil Régional de Bourgogne (via the 3MIM project), and the Agence Nationale de la Recherche (ANR-10-JCJC-0709) for funding.

REFERENCES

(1) Moyzis, R. K.; Buckingham, J. M.; Cram, L. S.; Dani, M.; Deaven, L. L.; Jones, M. D.; Meyne, J.; Ratliff, R. L.; Wu, J.-R. *Proc. Natl. Acad. Sci. U.S.A.* **1988**, *85*, 6622.

(2) Blackburn, E. H.; Gall, J. G. *J. Mol. Biol.* **1978**, *120*, 33.

(3) (a) de Lange, T. *Genes Dev.* **2005**, *19*, 2100. (b) Shay, J. W.; Wright, W. E. *Carcinogenesis* **2005**, *26*, 867. (c) Palm, W.; de Lange, T. *Annu. Rev. Genet.* **2008**, *42*, 301. (d) Giraud-Panis, M.-J.; Pisano, S.; Poulet, A.; Le Du, M.-H.; Gilson, E. *FEBS Lett.* **2010**, *584*, 3785. (e) Gilson, E.; Ségal-Bendirjian, E. *Biochimie* **2010**, *92*, 321.

(4) (a) Burge, S.; Parkinson, G. N.; Hazel, P.; Todd, A. K.; Neidle, S. *Nucleic Acids Res.* **2006**, *34*, 5402. (b) Patel, D. J.; Phan, A. T.; Kuryavyi, V. *Nucleic Acids Res.* **2007**, *35*, 7429. (c) Neidle, S. *Curr. Opin. Struct. Biol.* **2009**, *19*, 239. (d) Yang, D.; Okamoto, K. *Future Med. Chem.* **2010**, *2*, 619.

(5) (a) De Cian, A.; Lacroix, L.; Douarre, C.; Temime-Smaali, N.; Trentesaux, C.; Riou, J.-F.; Mergny, J.-L. *Biochimie* **2008**, *90*, 131. (b) Monchaud, D.; Teulade-Fichou, M.-P. *Org. Biomol. Chem.* **2008**, *6*, 627. (c) Balasubramanian, S.; Neidle, S. *Curr. Opin. Chem. Biol.* **2009**, *13*, 345. (d) Xu, Y. *Chem. Soc. Rev.* **2010**, *40*, 2719. (e) Neidle, S. *FEBS J.* **2010**, *277*, 1118.(f) Collie, G. W.; Parkinson, G. N. *Chem. Soc. Rev.* **2011**, *40*, 5867.

(6) (a) Beissenhirtz, M. K.; Willner, I. *Org. Biomol. Chem.* **2006**, *4*, 3392. (b) Teller, C.; Willner, I. *Curr. Opin. Biotechnol.* **2010**, *21*, 376. (c) Krishnan, Y.; Simmel, F. *Angew. Chem., Int. Ed.* **2011**, *50*, 3124.

(7) Silverman, S. K. *Angew. Chem., Int. Ed.* **2010**, *49*, 7180.

(8) Willner, I.; Shlyahocsky, B.; Zayats, M.; Willner, B. *Chem. Soc. Rev.* **2008**, *37*, 1153.

(9) (a) Travascio, P.; Li, Y.; Sen, D. *Chem. Biol.* **1998**, *5*, 505. (b) Travascio, P.; Bennet, A. J.; Wang, D. Y.; Sen, D. *Chem. Biol.* **1999**, *6*, 779.

(10) For detection of Cu^{2+}: (a) Yin, B.-C.; Ye, B.-C.; Tan, W.; Wang, H.; Xie, C.-C. *J. Am. Chem. Soc.* **2009**, *131*, 14624. For detection of Hg^{2+}: (b) Li, T.; Dong, S.; Wang, E. *Anal. Chem.* **2009**, *81*, 2144. (c) Kong, D.-M.; Wang, N.; Guo, X.-X.; Shen, H.-X. *Analyst* **2010**, 545. (d) Jia, S.-M.; Liu, X.-F.; Li, P.; Kong, D.-M.; Shen, H.-X. *Biosens. Bioelectron.* **2011**, *27*, 148. For detection of Pb^{2+}:(e) Elbaz, J.; Shlyahovsky, B.; Willner, I. *Chem. Commun.* **2008**, 1569. (f) Li, T.; Wang, E.; Dong, S. *Anal. Chem.* **2010**, *82*, 1515. (g) Lan, T.; Furuya, K.; Lu, Y. *Chem. Commun.* **2010**, 3896. (h) Yang, X.; Xu, J.; Tang, X.; Liu, H.; Tian, D. *Chem. Commun.* **2010**, 3107. (i) Li, T.; Dong, S.; Wang, E. *J. Am. Chem. Soc.* **2010**, *132*, 13156. (j) Li, C. L.; Liu, K. T.; Lin, Y. W.; Chang, T. H. *Anal. Chem.* **2011**, *83*, 225. (k) Lin, Z.; Li, X.; Kraatz, H. B. *Anal. Chem.* **2011**, *83*, 6896. For detection of K^+:(l) Li, T.; Wang, E.; Dong, S. *Chem. Commun.* **2009**, 580. (m) Yang, X.; Li, T.; Li, B.; Wang, E. *Analyst* **2010**, 71. For detection of Ag^+:(n) Zhou, X.-H.; Kong, D.-M.; Shen, H.-X. *Anal. Chem.* **2010**, *82*, 789. (o) Kong, D.-M.; Cai, L.-L.; Shen, H.-X. *Analyst* **2010**, 1253. (p) Zhou, X.-H.; Kong, D.-M.; Shen, H.-X. *Anal. Chim. Acta* **2010**, *678*, 124.

(11) For detection of nucleolin: (a) Li, T.; Shi, L.; Wang, E.; Dong, S. *Chem.-Eur. J.* **2009**, *15*, 1036. For detection of lysozyme:(b) Li, D.; Shlyahovsky, B.; Elbaz, J.; Willner, I. *J. Am. Chem. Soc.* **2007**, *129*, 5804. For detection of thrombin:(c) Li, T.; Wang, E.; Dong, S. *Chem.*

Commun. **2008**, 3654. (d) Zhu, J.; Li, T.; Hu, J.; Wang, E. *Anal. Bioanal. Chem.* **2010**, *397*, 2923. (e) Zhang, Y.; Li, B.; Jin, Y. *Analyst* **2011**, *136*, 3268.

(12) For detection of single-stranded DNA: (a) Weizmann, Y.; Beissenhirtz, M. K.; Cheglakov, Z.; Nowarski, R.; Kotler, M.; Willner, I. *Angew. Chem., Int. Ed.* **2006**, *45*, 7384. For detection of DNA/RNA analytes:(b) Weizmann, Y.; Cheglakov, Z.; Willner, I. *J. Am. Chem. Soc.* **2008**, *130*, 17224. (c) Nakayama, S.; Sintim, H. O. *J. Am. Chem. Soc.* **2009**, *131*, 10320. For detection of adenosine:(d) Sun, C.; Liu, X.; Feng, K.; Jiang, J.; Shen, G.; Yu, R. *Anal. Chim. Acta* **2010**, *669*, 87. For detection of single-nucleotide polymorphism:(e) Deng, M.; Zhang, D.; Zhou, Y.; Zhou, X. *J. Am. Chem. Soc.* **2008**, *130*, 13095. For detection of single-base mutations:(f) Willner, I.; Cheglakov, Z.; Weizmann, Y.; Sharon, E. *Analyst* **2008**, 923.

(13) Zhu, X.; Cao, Y.; Liang, Z.; Li, G. *Protein Cell* **2010**, *1*, 842.

(14) For the development of assays for screening G-quadruplex ligands: (a) Kong, D.-M.; Wu, J.; Ma, Y.-E.; Shen, H.-X. *Analyst* **2008**, *133*, 1158. (b) Chen, X.; Liu, X.; Bing, T.; Cao, Z.; Shangguan, D. *Biochemistry* **2009**, *48*, 7817. For the development of antioxidant assay: (c) Wang, M.; Han, Y.; Nie, Z.; Lei, C.; Huang, Y.; Guo, M.; Yao, S. *Biosens. Bioelectron.* **2010**, *26*, 523. (d) For the development of immunohistochemical assay: Thirstrup, D.; Baird, G. S. *Anal. Chem.* **2010**, *82*, 2498.

(15) (a) Li, T.; Wang, E.; Dong, S. *J. Am. Chem. Soc.* **2009**, *131*, 15082. (b) Shlyahovsky, B.; Li, Y.; Lioubashevski, O.; Elbaz, J.; Willner, I. *ACS Nano* **2009**, *3*, 1831. (c) Bi, S.; Yan, Y.; Hao, S.; Zhang, S. *Angew. Chem., Int. Ed.* **2010**, *49*, 4438. (d) Zhu, J.; Li, T.; Zhang, L.; Dong, S.; Wang, E. *Biomaterials* **2011**, *32*, 7318.

(16) (a) Pavlov, V.; Xiao, Y.; Gill, R.; Dishon, A.; Kotler, M.; Willner, I. *Anal. Chem.* **2004**, *76*, 2152. (b) Xiao, Y.; Pavlov, V.; Niazov, T.; Dishon, A.; Kotler, M.; Willner, I. *J. Am. Chem. Soc.* **2004**, *126*, 7430. (c) Freeman, R.; Sharon, E.; Teller, C.; Henning, A.; Tzfati, Y.; Willner, I. *ChemBioChem* **2010**, *11*, 2362.

(17) (a) Blackburn, E. H.; Greider, C. W.; Szostak, J. W. *Nat. Med.* **2006**, *12*, 1133. (b) Szostak, J. W. *Angew. Chem., Int. Ed.* **2010**, *49*, 7387. (c) Blackburn, E. H. *Angew. Chem., Int. Ed.* **2010**, *49*, 7405. (d) Greider, C. W. *Angew. Chem., Int. Ed.* **2010**, *49*, 7422.

(18) Morin, G. B. *Cell* **1989**, *59*, 521.

(19) Greider, C. W.; Blackburn, E. H. *Cell* **1985**, *43*, 405.

(20) Yu, H.-Q.; Miyoshi, D.; Sugimoto, N. *J. Am. Chem. Soc.* **2006**, *128*, 15461.

(21) Bauer, L.; Tluckova, K.; Tothova, P.; Viglasky, V. *Biochemistry* **2011**, *50*, 7484.

(22) (a) Haider, S.; Parkinson, G. N.; Neidle, S. *Biophys. J.* **2008**, *95*, 296. (b) Petraccone, L.; Trent, J. O.; Chaires, J. B. *J. Am. Chem. Soc.* **2008**, *130*, 16530. (c) Haider, S.; Neidle, S. *Biochem. Soc. Trans.* **2009**, *37*, 583. (d) Petraccone, L.; Garbett, N. C.; Chaires, J. B.; Trent, J. O. *Biopolymers* **2010**, *93*, 533.

(23) Xu, Y.; Ishizuka, T.; Kurabayashi, K.; Komiyama, M. *Angew. Chem., Int. Ed.* **2009**, *48*, 7833.

(24) Hazel, P.; Parkinson, G. N.; Neidle, S. *J. Am. Chem. Soc.* **2006**, *128*, 5480.

(25) (a) Shinohara, K.-i.; Sannohe, Y.; Kaieda, S.; Tanaka, K.-i.; Osuga, H.; Tahara, H.; Xu, Y.; Kawase, T.; Bando, T.; Sugiyama, H. *J. Am. Chem. Soc.* **2010**, *132*, 3778. (b) Cummaro, A.; Fottichia, I.; Franceschin, M.; Giancola, C.; Petraccone, L. *Biochimie* **2011**, *93*, 1392.

(26) Stefan, L.; Guédin, A.; Amrane, S.; Smith, N.; Denat, F.; Mergny, J.-L.; Monchaud, D. *Chem. Commun.* **2011**, *47*, 4992.

(27) Stefan, L.; Xu, H.-J.; Gros, C. P.; Denat, F.; Monchaud, D. *Chem.-Eur. J.* **2011**, *17*, 10857.

(28) Mergny, J.-L.; Li, J.; Lacroix, L.; Amrane, S.; Chaires, J. B. *Nucleic Acids Res.* **2005**, *33*, e138.

(29) (a) Gray, D. M.; Wen, J.-D.; Gray, C. W.; Repges, R.; Repges, C.; Raabe, G.; Fleischhauer, J. *Chirality* **2008**, *20*, 431. (b) Lane, A. N.; Chaires, J. B.; Gray, R. D.; Trent, J. O. *Nucleic Acids Res.* **2008**, *36*, 5482.

(30) Dai, J.; Carver, M.; Punchihewa, C.; Jones, R. A.; Yang, D. *Nucleic Acids Res.* **2007**, *37*, 4927.

(31) Zhu, X.; Gao, X.; Liu, Q.; Lin, Z.; Qiu, B.; Chen, G. *Chem. Commun.* **2011**, *47*, 7437.

(32) De Cian, A.; Guittat, L.; Kaiser, M.; Saccà, B.; Amrane, S.; Bourdoncle, A.; Alberti, P.; Teulade-Fichou, M.-P.; Lacroix, L.; Mergny, J.-L. *Methods* **2007**, *42*, 183.

(33) (a) Nikan, M.; Sherman, J. C. *Angew. Chem., Int. Ed.* **2008**, *47*, 4900. (b) Nikan, M.; Sherman, J. C. *J. Org. Chem.* **2009**, *74*, 5211. (c) Murat, P.; Bonnet, R.; Van der Heyden, A.; Spinelli, N.; Labbé, P.; Monchaud, D.; Teulade-Fichou, M.-P.; Dumy, P.; Defrancq, E. *Chem. Eur. J.* **2010**, *16*, 6106. (d) Murat, P.; Gennaro, B.; Garcia, J.; Spinelli, N.; Dumy, P.; Defrancq, E. *Chem.-Eur. J.* **2011**, *17*, 5791.